Liu et al. Supplementary Figure 1

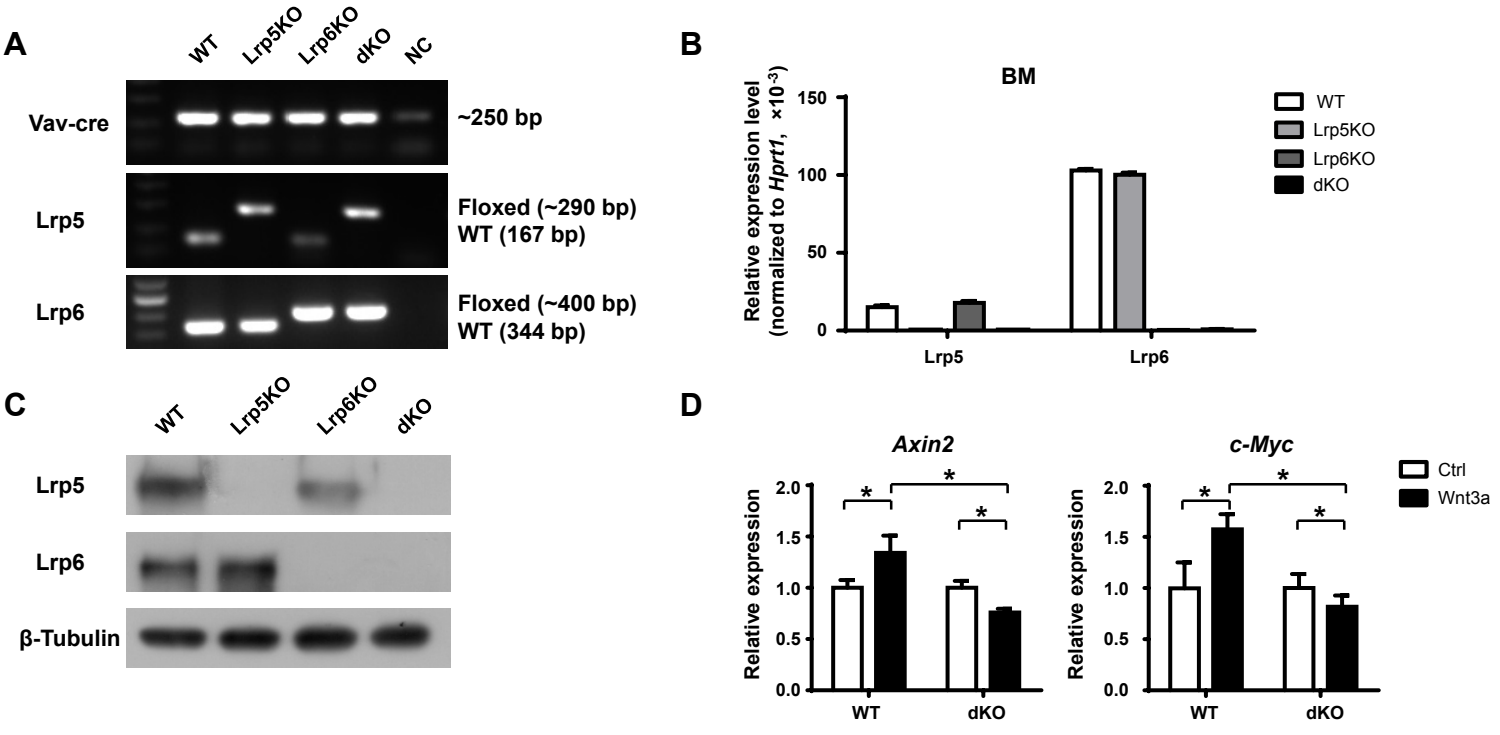

Figure S1. Characterization of Lrp5 and Lrp6 knockout mice.

(A) Genotyping of the wild-type (*Vav*-Cre), Lrp5KO (*Lrp5*$^{fl/fl}$*Lrp6*$^{+/+}$*Vav*-Cre), Lrp6KO (*Lrp5*$^{+/+}$*Lrp6*$^{fl/fl}$ *Vav*-Cre) and dKO (*Lrp5*$^{fl/fl}$*Lrp6*$^{fl/fl}$*Vav*-Cre**)** mice with genomic DNA. The product size of *Vav*-Cre was appropriately 250 bp. The product sizes of Lrp5 were 167 bp from WT allele and 290 bp from floxed allele, respectively. The product sizes of Lrp6 were 344 bp from WT allele and about 400 bp from floxed allele, respectively. **(B)** Quantitative RT-PCR analysis of Lrp5 and Lrp6 expression in BM cells from wild-type, Lrp5KO, Lrp6KO and dKO mice. Relative gene expression levels were normalized to *Hprt1*. **(C)** Western blotting analysis of Lrp5 and Lrp6 expression in BM cells from wild-type, Lrp5KO, Lrp6KO and dKO mice. β-tubulin were set as an internal control. **(D)** Analysis of the canonical Wnt pathway activation. Lin$^-$ BM cells were treated with rmWnt3a (40 ng/ml) and Wnt target genes *Axin2* and *c-Myc* were detected by quantitative RT-PCR. Relative gene expression levels were normalized to *Hprt1*. Data are representative of at least two independent experiments (means ± S.D.). ($n \geq 4$). *$p < 0.05$, by Student's *t* test.

Liu et al. Supplementary Figure 2

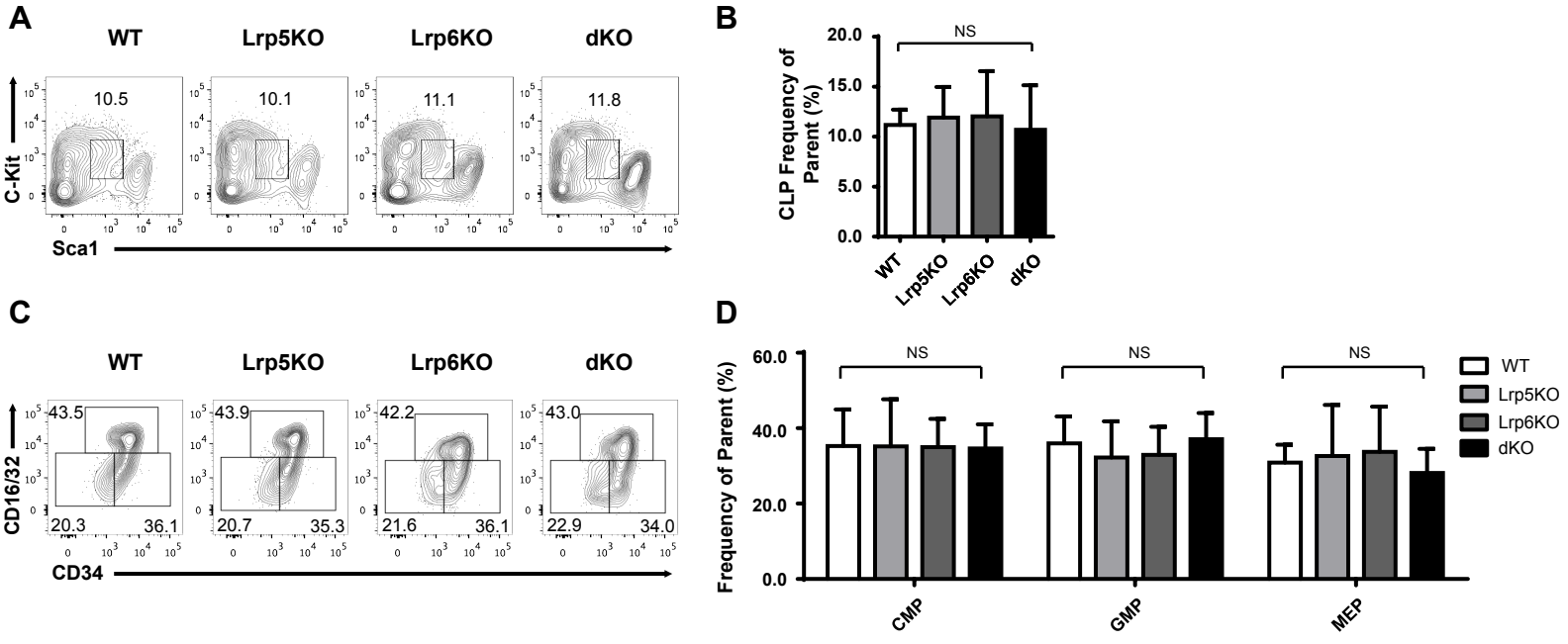

Figure S2. Characterization of progenitor cells in Lrp5 and Lrp6 KO mice.

(A-B) Flow cytometry analysis of CLP ($Lin^{-}CD127^{+}Sca\text{-}1^{med}c\text{-}kit^{med}$). The percentages of CLP are shown in representative contour plots **(A).** Cumulative data of CLP are shown in **(B). (C-D)** Flow cytometry analysis of CMP, GMP, and MEP. BMs were surface stained by CD34 and CD16/32 to identify CMP ($CD34^{+}CD16/32^{lo}$), GMP ($CD34^{+}CD16/32^{hi}$) and MEP ($CD34^{-}CD16/32^{lo}$). The percentages of each cell subsets are shown in representative contour plots **(C).** Cumulative data of CMP, GMP and MEP are shown in **(D).** Data are representative of four independent experiments (means ± S.D.) ($n \geq 6$) NS, not significant, by Student's *t* test.

Liu et al. Supplementary Figure 3

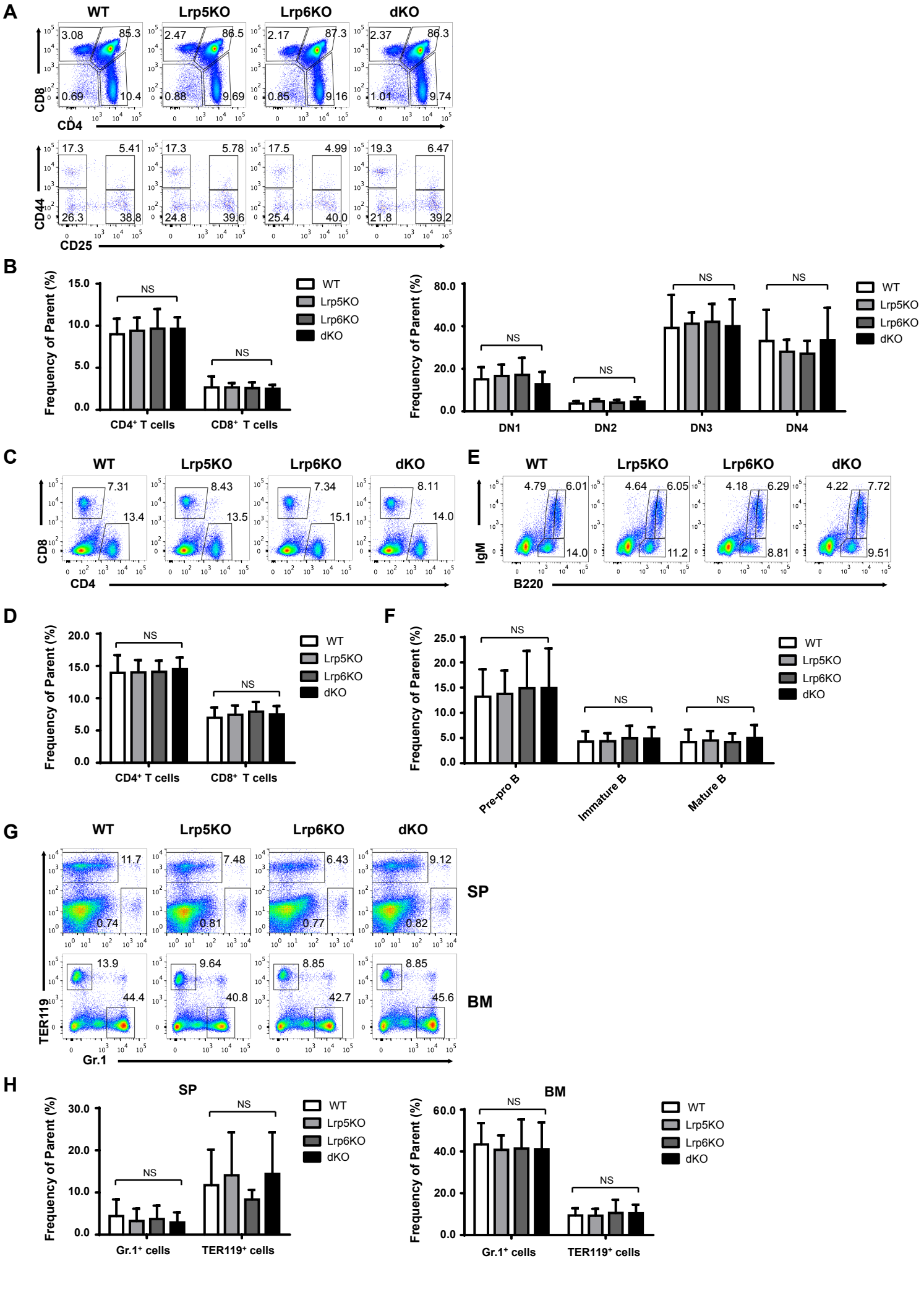

Figure S3. Detection of the lymphoid and myeloid cells in Lrp5 and Lrp6 KO mice. **(A-B)** Flow cytometry analysis of T cell development. Thymocytes from indicated mice were surface stained with CD4, CD8, CD44, and CD25. The percentages of each cell subsets were shown in representative pseudocolor plots (**A**). Cumulative data of $CD4^+$ single positive T cells, $CD8^+$ single positive T cells and DN1 ($lin^-CD4^-CD8^-CD44^+CD25^-$ thymocytes), DN2 ($lin^-CD4^-CD8^-CD44^+CD25^+$ thymocytes), DN3 ($lin^-CD4^-CD8^-CD44^-CD25^+$ thymocytes), and DN4 ($lin^-CD4^-CD8^-CD44^-CD25^-$ thymocytes) cells are shown in (**B**) ($n \geq 12$). (**C-D**) Flow cytometry analysis of splenic T cells. Splenocytes were surface stained with CD4 and CD8. The percentages of indicated cell subsets are shown in representative pseudocolor plots (**C**). Cumulative data of indicated cells are shown in (**D**) ($n \geq 12$). (**E-F**) Flow cytometry analysis of B cell development. BM cells were surface stained with B220 and IgM. The percentages of indicated cell subsets are shown in representative pseudocolor plots (**E**). Cumulative data of indicated cells are shown in (**F**) ($n \geq 14$). (**G-H**) Flow cytometry analysis of $Gr.1^+$ and $Ter119^+$ cell populations in spleen and BM cells. Splenocytes and BM cells were surface stained with Gr.1 and Ter119. The percentages of $Gr.1^+$ and $Ter119^+$ cells are shown in representative pseudocolor plots (**G**). Cumulative data of $Gr.1^+$ and $Ter119^+$ cells are shown in (**H**). Data are representative of four (**G-H**), five (**A-D**) or six (**E-F**) independent experiments (means ± S.D.) ($n \geq 8$). NS, not significant, by Student's *t* test.

Liu et al. Supplementary Tables

Table 1 Primers for genotyping

Primer	Sequence (5'→3')
Lrp5-Type-F	TCACCTGTCCTAGTGCAGAAGGA
Lrp5-Type-R	CCACCAATCATCAGCCAAGGA
Lrp6-Type-F	CCGTCTGTTTGCATAAAGCAACA
Lrp6-Type-R	GGGGTTCTACTTTTGTGTGTGG
Vav1-cre-F	AGATGCCAGGACATCAGGAACCTG
Vav1-cre-R	ATCAGCCACACCAGACACAGAGATC

Table 2 Primers for quantitative RT-PCR

Primer	Sequence (5'→3')
RT-Axin2-F	AAGAGAAGCGACCCAGTCAA
RT-Axin2-R	CTGCGATGCATCTCTCTCTG
RT-Btg2-F	ATGAGCCACGGGAAGAGAAC
RT-Btg2-R	GCCCTACTGAAAACCTTGAGTC
RT-Ccna2-F	CAGCATGAGGGCCATCCTT
RT-Ccna2-R	GCAGGGTCTCATTCTGTAGTTTATATTCT
RT-Cdkn1a-F	GCAGATCCACAGCGATATCCAG
RT-Cdkn1a-R	GAGGAAGTACTGGGCCTCTTGT
RT-c-Myc-F	GTACCTCGTCCGATTCCACG
RT-c-Myc-R	GCCTCTTCTCCACAGACACC
RT-Egr1-F	GAGCGAACAACCCTATGAGC

RT-Egr1-R	GAGTCGTTTGGCTGGGATAA
RT-GAPDH-F	CTTCAACAGCAACTCCCACTC
RT-GAPDH-R	CCTGTTGCTGTAGCCGTATTC
RT-Gata2-F	GCTTCACCCCTAAGCAGAGA
RT-Gata2-R	TGGCACCACAGTTGACACA
RT-Hprt1-F	GCGTCGTGATTAGCGATGATG
RT-Hprt1-R	CTCGAGCAAGTCTTTCAGTCC
RT-Junb-F	TCACGACGACTCTTACGCAG
RT-Junb-R	CCTTGAGACCCCGATAGGGA
RT-Lef1-F	TGAGTGCACGCTAAAGGAGA
RT-Lef1-R	CTGACCAGCCTGGATAAAGC
RT-LRP5-F	GGACGTCCCGTAAGGTTCTC
RT-LRP5-R	CCATTGGGCCAGTAAATGTC
RT-LRP6- F	GAGTTGGATCAACCCAGAGC
RT-LRP6- R	GTCAGTCCGTTTGGCCAGTA
RT-Nr4a1-F	TTGAGTTCGGCAAGCCTACC
RT-Nr4a1-R	GTGTACCCGTCCATGAAGGTG
RT-Ranbp1-F	CGAGGACCATGATACTTCCACA
RT-Ranbp1-R	CCTCCAGCGTTTTAATTTCTTGC
RT-Ran-F	CCACTTGACGGGCGAGTTT
RT-Ran-R	CCACACAATACAATGGGGATGTT